AC vs. DC Boost Converters: A Detailed Conduction Loss Comparison

Daniel L Gerber
Building Technology and Urban Systems
Lawrence Berkeley Labs
Berkeley, CA, USA
dgerb@lbl.gov

Fariborz Musavi
Engineering and Computer Science
Washington State University
Vancouver, WA, USA
fariborz.musavi@wsu.edu

***Abstract*—Studies have shown the efficiency benefits of DC distribution systems are largely due to the superior performance of DC/DC converters. Nonetheless, these studies are often based on product data that differs widely in manufacturer and operating voltage. This work develops a rigorous loss model to theoretically compare the efficiency of a DC/DC and an AC/DC PFC boost converter. It ensures each converter has the same components and equivalent operating voltages. The results show AC boost converters below 500 W to have 2.9 to 4.2 times the loss of DC.**

Keywords—DC microgrid, boost converter, loss model, power factor correction

I. Introduction and Motivation

Direct current (DC) distribution has taken the spotlight in microgrid research due to the proliferation of solar generation, battery storage, and internally-DC loads. Recent studies and experiments compare the system efficiency of an AC and DC microgrid [1]–[8]. For the commercial building sector, the reported savings with DC vary widely from 2% [1] to as much as 19% [8]. In general, the reported savings are highly dependent on the system converter efficiencies, the system topology and voltage levels, and the coincidence of generation and load. In 2017, Gerber et al. performed a series of highly-detailed parametric simulations that varied solar and storage capacity in equivalent AC and DC buildings. An extensive loss analysis revealed low-power AC/DC converters to contribute the most loss in AC buildings [3]. For example, the peak efficiency of a high-quality AC/DC LED driver is 94%, whereas a DC/DC LED driver is typically 98% [4].

These studies have many limitations, the most significant being nonequivalent models for AC and DC converters. These models often use efficiency curves from product data, which can be limited or biased, especially for the less-common DC products. In addition, previous studies compare AC and DC systems at very different distribution voltages (AC 120 V_{rms} or 480 V_{rms}, and DC 48 V or 380 V). Such a comparison favors the system with the higher distribution voltage, since high-voltage converters tend to be more efficient. Ideally, these studies would compare AC and DC systems at the same voltage, but it would be difficult to find product data for one of the systems.

This work develops a rigorous loss model to theoretically compare the efficiency of equivalent AC and DC converters at the same voltage. Although several previous works have analyzed and established loss models for the DC/DC [9]–[12] and AC/DC PFC [13]–[20] boost converters, they each have their own methods and formulae, making an analytic comparison difficult. In addition, many of them neglect essential components such as the input bridge drop and output capacitor equivalent series resistance (ESR). This is the first work to establish a set of formulae that compare the loss between an AC and DC boost converter, both of which have the same components and equivalent operating voltages. Although DC/DC converters are already known to be more efficient, this work reports exactly how much more.

U.S. Department of Energy Contract No. DE-AC02-05CH11231

II. Deriving Switching Converter Loss Models

This work models the resistive and diode loss elements in the boost converter. The process requires solving for the average and RMS currents through each component. As shown in Figure 1, these include the inductor ($I_{L,rms}$), switch ($I_{Q,rms}$), boost diode ($I_{D,rms}$, $I_{D,ave}$), output capacitor ($I_{C,rms}$), and the two active bridge diodes ($I_{B,rms}$, $I_{B,ave}$). The average resistive loss $P_{Loss,R}$ in the inductor, switch, and capacitor is modeled as

$$P_{Loss,R} = R_R * I_{rms}^2, \tag{1}$$

where R_R is the inductor copper resistance, switch on-state resistance, or capacitor ESR, respectively. The average diode loss $P_{Loss,D}$ in the boost and bridge diodes is approximated as a fixed diode drop V_D and series resistor R_D:

$$P_{Loss,D} = V_D * I_{ave} + R_D * I_{rms}^2. \tag{2}$$

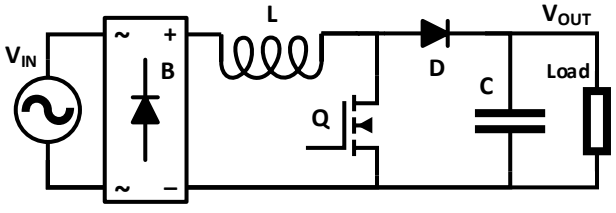

Fig. 1: The AC PFC boost converter model includes the input inductor L, two of the bridge diodes B, the switch Q, the boost diode D, and the output capacitor C. The DC boost converter has an input at the inductor, and bypasses the diode bridge.

The converter's total average conduction loss is the sum of P_{Loss} over all components.

In order to determine the component currents, the loss model requires several assumptions [13], [14]:

- The converter operates in continuous conduction mode
- The boost PFC line current is perfectly in phase with the line voltage
- The output voltage is DC, and the output capacitor completely absorbs the output power ripple
- The converter operates at 100% efficiency ($P_{in} = P_o$)
- This analysis does not cover switching and gate-drive losses, which are expected to be similar between the AC and DC boost converters anyway

The average and RMS values of the component currents are both found by integrating the current waveform. As shown in Figure 2a, the component currents of the AC boost vary with the low-frequency AC angle θ, and require an outer integral over $\theta = 0$ to π. They also vary over the high-frequency switching period T. As shown in Figure 2b, θ is approximately constant at the switching time scale, and the currents are integrated over a single switching period $t = 0$ to T. For any RMS calculations,

$$i_{rms,t}(\theta) = \sqrt{\int_0^T i^2(\theta, t)dt} \tag{3}$$

$$I_{rms} = \sqrt{\int_0^\pi i^2_{rms,t}(\theta)d\theta} \tag{4}$$

where $i(\theta, t)$ is the instantaneous current and $i_{rms,t}(\theta)$ is the switching-period RMS. The DC boost has a constant θ, and so $I_{rms} = i_{rms,t}(\theta)$ for DC.

Integration over T can be solved via geometric methods. As shown in Figure 2b, the component currents are represented as either a bilateral triangle (i_L, i_B) or an elevated right triangle (i_Q, i_D, i_C). In this analysis, the bilateral triangle Δ^B is zero-centered and not necessarily isosceles. Its average and RMS are

$$\Delta^B_{avg,t} = 0 \tag{5}$$

$$\Delta^B_{rms,t}(A) = \frac{A}{2\sqrt{3}}, \tag{6}$$

where A is the triangle's peak-to-peak height, shown in Figure 2c. The average and RMS of the elevated right triangle Δ^R are

$$\Delta^R_{avg,t}(B, D) = BD \tag{7}$$

$$\Delta^R_{rms,t}(A, B, D) = \frac{\sqrt{D}}{2\sqrt{3}}\sqrt{A^2 + 12B^2}, \tag{8}$$

where A is the height of the triangular section, B is the elevation of the triangle's midpoint, and D is the duty cycle for which the component is active. As shown in Equations (5) and (7), the average is independent from A, and thus is unaffected by current ripple.

For each converter, this work develops two models: a simple model and a model that accounts for inductor-current

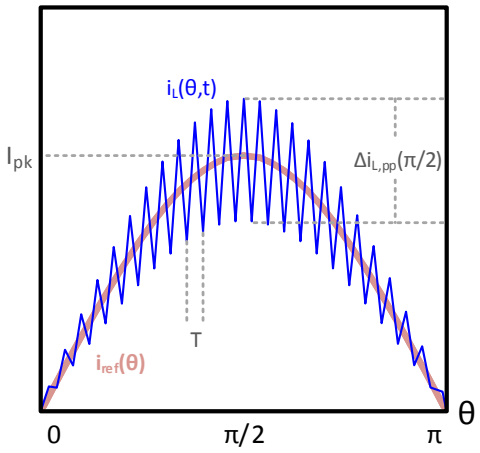

(a) The inductor current $i_L(\theta, t)$ tracks the input current reference $I_{ref}(\theta) = I_{pk}sin(\theta)$.

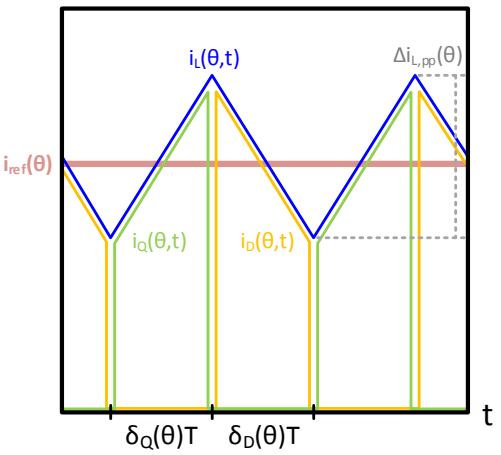

(b) On the switching timescale, θ is approximately constant. The $i_L(\theta, t)$ passes through the switch (green) during $\delta_Q(\theta)$, and the boost diode (orange) during $\delta_D(\theta)$.

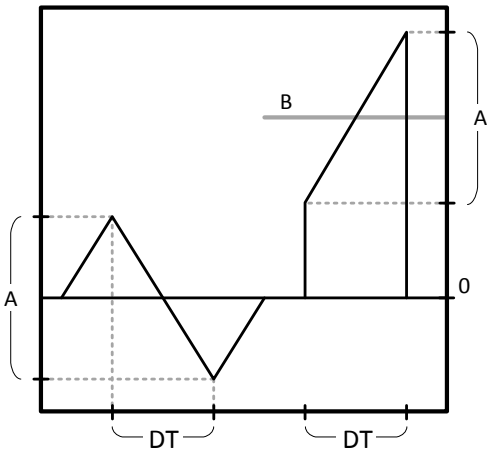

(c) These triangle functions represent the current waveforms for several components. The bilateral triangle Δ^B (left) represents the inductor ripple. The elevated right triangle Δ^R (right) is useful for the switch and boost diode.

Fig. 2: Waveforms and triangles relevant to the analysis.

ripple. In each case, the component currents can be derived from Δ^B or Δ^R. The simple model ignores the inductor-current ripple and assumes $A = 0$, which simplifies many of the expressions without much loss of accuracy.

Finally, it is important to note that the RMS of orthogonal waveforms can be combined. For example, if $i_1(t)$ and $i_2(t)$ are orthogonal and $i(t) = i_1(t) + i_2(t)$, then

$$I_{rms} = \sqrt{I_{rms,1}^2 + I_{rms,2}^2}. \tag{9}$$

III. Boost Converter Component Currents

A. Input and Duty Cycle

This work compares AC and DC boost converters at equivalent voltage and power levels. While both converters operate at the same constant output voltage V_o and power P_o, they have different inputs. The AC and DC inputs are

$$v_{i,AC}(\theta) = V_{pk} sin(\theta) \tag{10}$$

$$i_{ref,AC}(\theta) = I_{pk} sin(\theta) = \frac{2P_o}{V_{pk}} sin(\theta) \tag{11}$$

$$v_{i,DC} = V_{pk} \tag{12}$$

$$i_{ref,DC} = \frac{P_o}{V_{pk}}. \tag{13}$$

The equivalent DC input voltage is established as the peak of the sinusoidal AC input. This is a fair comparison, since most application-relevant input specifications depend on the peak voltage (e.g. breakdown, stress, insulation, safety, etc.). As such, the DC input current will be generally lower than the AC input. Note that θ is constant for the DC converter.

The triangle formulae in Equations (5) to (8) also require the switching duty cycle. It is convenient to separately express the duty cycle for the switch δ_Q, and the boost diode δ_D:

$$\delta_Q(\theta) = 1 - \frac{v_i(\theta)}{V_o} \tag{14}$$

$$\delta_D(\theta) = \frac{v_i(\theta)}{V_o}. \tag{15}$$

The following sections will explain how to calculate the average and RMS currents for each component. The final expressions for the RMS and average currents are collected in Table I for the simple model, and Table II for the model with ripple.

B. Inductor Current

1) Simple Model: As shown in Figure 2a, the input inductor current of a boost PFC is approximately equal to i_{ref} when ripple is ignored. As such, the RMS inductor current $i_{L,rms}$ is simply the RMS of i_{ref}. The final expression for $I_{L,rms}$ is in Table I.

2) Model with Ripple: The RMS inductor current increases when current ripple is accounted for. Inductor ripple appears as the bilateral triangle shown in Figure 2c, with a peak-to-peak ripple $i_{L,pp}(\theta)$ of

$$\Delta i_{L,pp}(\theta) = \frac{v_i(\theta)\delta_Q(\theta)}{fL}. \tag{16}$$

The inductor ripple RMS $\Delta i_{L,rms}$ can then be solved from Equations (4) and (6) as

$$\Delta i_{L,rms,t}(\theta) = \Delta^B_{rms}(A = \Delta i_{L,pp}(\theta)) \tag{17}$$

$$\Delta I_{L,rms} = \sqrt{\int_0^\pi i^2_{L,rms,t}(\theta) d\theta}. \tag{18}$$

As shown in Figure 2a, the inductor current $i_L(\theta, t)$ in a boost PFC is the sum of $i_{ref}(\theta)$ and the ripple function $\Delta i_L(\theta, t)$. These two functions are essentially orthogonal, and may be combined as per Equation (9):

$$I_{L,rms} = \sqrt{I^2_{ref,rms} + \Delta I^2_{L,rms}}, \tag{19}$$

The final expression for $I_{L,rms}$ is in Table II.

C. Diode Bridge Current

1) Simple Model: The instantaneous diode bridge current always equals that of the inductor, therefore $I_{B,rms} = I_{L,rms}$. In the simple model, $i_B(\theta, t) = i_{ref}(\theta)$, and the average bridge current $I_{B,avg}$ is the average of $i_{ref}(\theta)$.

2) Model with Ripple: As shown in Equation (5), the average ripple of a bilateral triangle is zero. Even with ripple, $I_{B,avg}$ still equals its simple-model value.

D. Switch Current

1) Simple Model: The inductor current passes through the switch during $\delta_Q(\theta)$, as shown in Figure 2b. Both the simple and ripple models integrate the elevated right triangle $\Delta^R_{rms,t}$. The simple model assumes $A = 0$, and evokes Equations (4) and (8) to solve for the RMS switch current $I_{Q,rms}$:

$$I_{Q,rms,t}(\theta) = \Delta^R_{rms,t}(A = 0, B = i_{ref}(\theta), D = \delta_Q(\theta)). \tag{20}$$

2) Model with Ripple: To account for inductor ripple through the switch, evaluate Equation (8) with $A = \Delta i_{L,pp}(\theta)$.

E. Boost Diode Current

Both models of the boost diode solve for the RMS current using the analysis in Section III-D, except with $D = \delta_D(\theta)$. The average current is found by integrating $\Delta^R_{avg,t}$, and is the same for both models.

F. Capacitor Current

The capacitor current $i_C(\theta, t)$ is equal to the difference between the boost diode current $i_D(\theta, t)$ and the constant output current $\frac{P_o}{V_o}$. These currents are orthogonal, and by Equation (9),

$$I_{C,rms} = \sqrt{I^2_{D,rms} - (\frac{P_o}{V_o})^2} \tag{21}$$

for both models.

TABLE I: Simple model of component currents

Parameter	AC/DC PFC	DC/DC	min($P_{Loss,AC}/P_{Loss,DC}$)
$I_{L,rms}$ $I_{B,rms}$	$\frac{\sqrt{2}P_o}{V_{pk}}$	$\frac{P_o}{V_{pk}}$	2
$I_{B,avg}$	$\frac{4}{\pi}\frac{P_o}{V_{pk}}$	$--$	$--$
$I_{Q,rms}$	$\frac{P_o}{\sqrt{V_o V_{pk}}}\sqrt{2V_o - \frac{16}{3\pi}V_{pk}}$	$\frac{P_o}{\sqrt{V_o V_{pk}}}\sqrt{V_o - V_{pk}}$	2
$I_{D,rms}$	$\frac{4}{\sqrt{3}\pi}\frac{P_o}{\sqrt{V_o V_{pk}}}$	$\frac{P_o}{\sqrt{V_o V_{pk}}}$	$\frac{16}{3\pi} \approx 1.70$
$I_{D,avg}$	$\frac{P_o}{V_o}$	$\frac{P_o}{V_o}$	1
$I_{C,rms}$	$\frac{P_o}{V_o\sqrt{V_{pk}}}\sqrt{\frac{16}{3\pi}V_o - V_{pk}}$	$\frac{P_o}{V_o\sqrt{V_{pk}}}\sqrt{V_o - V_{pk}}$	$\frac{16}{3\pi} \approx 1.70$

TABLE II: Model of component currents with ripple

Parameter	AC/DC PFC	DC/DC
$I_{L,rms}$ $I_{B,rms}$	$\frac{\sqrt{576\pi L^2 P_o^2 V_o^2 + 12\pi T^2 V_o^2 V_{pk}^4 - 64T^2 V_o V_{pk}^5 + 9\pi T^2 V_{pk}^6}}{12LV_oV_{pk}\sqrt{2\pi}}$	$\frac{\sqrt{12L^2P_o^2V_o^2 + T^2V_o^2V_{pk}^4 - 2T^2V_oV_{pk}^5 + T^2V_{pk}^6}}{2LV_oV_{pk}\sqrt{3}}$
$I_{B,avg}$	$\frac{4P_o}{\pi V_{pk}}$	$--$
$I_{Q,rms}$	$\frac{\sqrt{2880\pi L^2 P_o^2 V_o^3 - 7680L^2P_o^2V_oV_{pk} + 60\pi T^2 V_o^3 V_{pk}^4 \cdots}}{12LV_{pk}\sqrt{10\pi V_o^3}}$ $\frac{\cdots - 480T^2V_o^2V_{pk}^5 + 135\pi T^2 V_o V_{pk}^6 - 128T^2V_{pk}^7}{}$	$\frac{\sqrt{\left(V_o - V_{pk}\right)\left(12L^2P_o^2V_o^2 + T^2V_o^2V_{pk}^4 - 2T^2V_oV_{pk}^5 + T^2V_{pk}^6\right)}}{2LV_{pk}\sqrt{3V_o^3}}$
$I_{D,rms}$	$\frac{\sqrt{3840L^2P_o^2V_o^2 + 80T^2V_o^2V_{pk}^4 - 45\pi T^2V_oV_{pk}^5 + 64T^2V_{pk}^6}}{12L\sqrt{5\pi V_o^3 V_{pk}}}$	$\frac{\sqrt{12L^2P_o^2V_o^2 + T^2V_o^2V_{pk}^4 - 2T^2V_oV_{pk}^5 + T^2V_{pk}^6}}{2L\sqrt{3V_o^3V_{pk}}}$
$I_{D,avg}$	$\frac{P_o}{V_o}$	$\frac{P_o}{V_o}$
$I_{C,rms}$	$\frac{\sqrt{3840L^2P_o^2V_o^2 - 720\pi L^2P_o^2V_oV_{pk} + 80T^2V_o^2V_{pk}^4 - 45\pi T^2V_oV_{pk}^5 + 64T^2V_{pk}^6}}{12L\sqrt{5\pi V_o^3V_{pk}}}$	$\frac{\sqrt{\left(V_o - V_{pk}\right)\left(12L^2P_o^2V_o + T^2V_oV_{pk}^4 - T^2V_{pk}^5\right)}}{2L\sqrt{3V_o^3V_{pk}}}$

G. Summary of Model Currents

Final expressions of all the component currents are given in Tables I and II for the simple and ripple models, respectively. In Table I, the leftmost column shows the ratio of loss power per component between equivalent AC and DC boost converters. For $I_{Q,rms}$ and $I_{C,rms}$, this ratio is minimized at very high V_o. RMS and average currents correspond to resistive and diode losses, respectively.

IV. Model Validation

This work validates the boost converter loss model through a transient PSIM 11.1.5 simulation over a 120 Hz period. The simulated boost converter is ideal, with either an AC/DC PFC or a DC/DC control loop. As shown in Tables III and IV, the simulation results closely match the model.

This work also validates the model with the experimental prototype in Figure 3. The prototype is designed for an output power $P_o = 250$ W, output voltage $V_o = 350$ V, and input voltage $V_{pk} = 170$ V. Its components, shown in Table V, are the same between AC and DC boost experiments. Tables III and IV show the experiment to be somewhat consistent with the model and simulation. As previously mentioned in Section II, the model only holds for prototypes with relatively high efficiency (>90%).

TABLE III: AC/DC PFC Boost Model Validation Currents (A): P_o = 250 W, V_o = 350 V, and V_{pk} = 170 V

Parameter	Model (simple)	Model (ripple)	Simulation	Experiment
$I_{L,rms}$ $I_{B,rms}$	2.153	2.161	2.162	2.356
$I_{B,avg}$	1.938	1.938	1.938	2.105
$I_{Q,rms}$	1.655	1.662	1.662	1.723
$I_{D,rms}$	1.376	1.381	1.382	1.323
$I_{D,avg}$	0.733	0.733	0.733	0.781
$I_{C,rms}$	1.165	1.171	1.171	$--$

V. AC vs DC Efficiency Comparison

This section presents a direct comparison between AC and DC boost converters using the loss models developed in Sections II and III. The analysis combines the component currents from Table II with real component parasitics in Table V. The overall loss is the sum of the component losses determined in Equations (1) and (2).

TABLE IV: DC/DC Boost Model Validation Currents (A): P_o = 250 W, V_o = 350 V, and V_{pk} = 170 V

Parameter	Model (simple)	Model (ripple)	Simulation	Experiment
$I_{L,rms}$ $I_{B,rms}$	1.466	1.485	1.485	1.552
$I_{B,avg}$	1.466	1.466	1.466	1.452
$I_{Q,rms}$	1.056	1.070	1.070	1.041
$I_{D,rms}$	1.017	1.030	1.030	1.105
$I_{D,avg}$	0.705	0.705	0.705	0.717
$I_{C,rms}$	0.732	0.751	0.751	– –

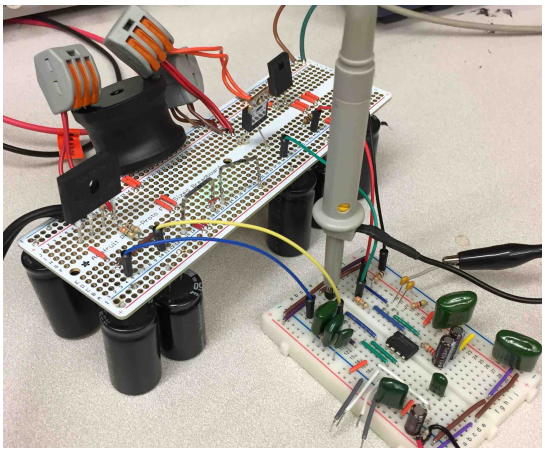

Fig. 3: Experimental prototype for a boost converter with $P_o = 250$ W, $V_o = 350$ V, and $V_{pk} = 170$ V.

The loss comparison is illustrated by the efficiency curves in Figure 4. The AC boost has 2.9 to 4.2 times the loss of the DC boost in the range of 100 W to 500 W. Note that this model does not account for switching loss, which would normally decrease the efficiency at low power. A loss analysis in Figure 5 reveals the switch and diode bridge to be the main sources of loss, given the components in Table V.

VI. Conclusion

System efficiency comparisons between AC and DC often fail to compare converters with equivalent voltages and components. This work develops a rigirous formula-based loss model to compare an AC and DC boost converter. The model is based on component currents, which are validated through both simulation and experiment. The results show AC boost converters below 500 W to have 2.9 to 4.2 times the loss of DC. Nonetheless, there are various other DC/DC topologies that are even more efficient than the boost, including resonant and switched-capacitor converters. Therefore, this study serves more as a baseline for an AC and DC comparison. Future work involves extending the comparison to other types of converters.

TABLE V: Components in Prototype

Component	Part Number	Parameters
Inductor (2x)	Bourns 1140-821K-RC	$R_R = 0.154$ (each inductor)
Diode Bridge	Diodes Inc. GBU804	$V_D = 1$ $R_D = 0.028$ (each diode)
Switch	Vishay IRF840PBF	$R_R = 0.85$
Boost Diode	Cree C3D04060F	$V_D = 0.81$ $R_D = 0.13$
Capacitor (10x)	TKD B43501A6107M000	$R_R = 1.33$ (each cap)
Boost PFC Controller	TI UCC28019	– –
Boost DCDC Controller	Arduino Uno	– –

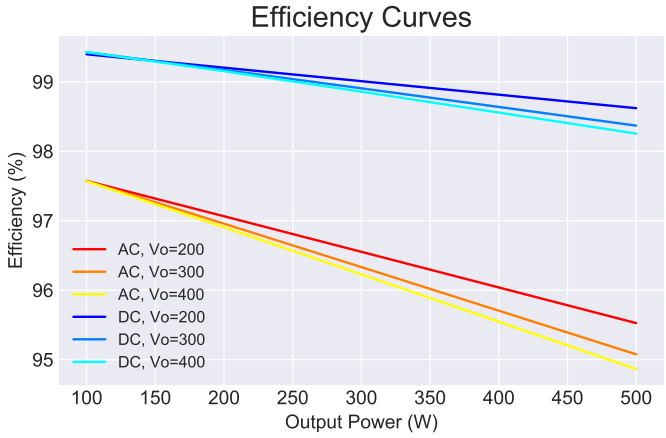

Fig. 4: Efficiency curves that compare an AC and DC boost converter with the same components and input voltage V_{pk} = 170 V. The model only accounts for conduction losses.

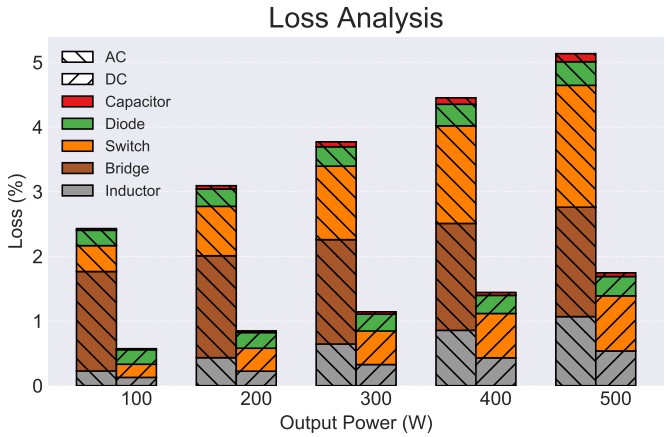

Fig. 5: Loss analysis for the AC and DC boost converters with input voltage V_{pk} = 170 V and output voltage V_o = 400 V.

ACKNOWLEDGMENT

This research is supported by Lawrence Berkeley National Laboratory through the U.S. Department of Energy under Contract No. DE-AC02-05CH11231 and the U.S. China Clean Energy Research Center, Building Energy Efficiency (CERC-BEE) program. The authors would like to thank Richard Brown, Richard Liou, and Wei Feng for their support.

REFERENCES

[1] S. Backhaus, G. W. Swift, S. Chatzivasileiadis, W. Tschudi, S. Glover, M. Starke, J. Wang, M. Yue, and D. Hammerstrom, "DC Microgrids Scoping Study Estimate of Technical and Economic Benefits," Tech. Rep. LAUR1522097, Los Alamos National Laboratory, Mar. 2015.

[2] D. Denkenberger, D. Driscoll, E. Lighthiser, P. May-Ostendorp, B. Trimboli, and P. Walters, "DC Distribution Market, Benefits, and Opportunities in Residential and Commercial Buildings," tech. rep., Pacific Gas & Electric Company, Oct. 2012.

[3] D. L. Gerber, V. Vossos, W. Feng, C. Marnay, B. Nordman, and R. Brown, "A simulation-based efficiency comparison of ac and dc power distribution networks in commercial buildings," *Applied Energy*, vol. 210, pp. 1167 – 1187, 2018.

[4] D. Fregosi, S. Ravula, D. Brhlik, J. Saussele, S. Frank, E. Bonnema, J. Scheib, and E. Wilson, "A comparative study of DC and AC microgrids in commercial buildings across different climates and operating profiles," in *2015 IEEE First International Conference on DC Microgrids (ICDCM)*, pp. 159–164, June 2015.

[5] G. AlLee and W. Tschudi, "Edison Redux: 380 Vdc Brings Reliability and Efficiency to Sustainable Data Centers," *IEEE Power and Energy Magazine*, vol. 10, pp. 50–59, Nov. 2012.

[6] R. Weiss, L. Ott, and U. Boeke, "Energy efficient low-voltage DC-grids for commercial buildings," in *2015 IEEE First International Conference on DC Microgrids (ICDCM)*, pp. 154–158, June 2015.

[7] A. Sannino, G. Postiglione, and M. Bollen, "Feasibility of a DC network for commercial facilities," *IEEE Transactions on Industry Applications*, vol. 39, pp. 1499–1507, Sept. 2003.

[8] P. Savage, R. R. Nordhaus, and S. P. Jamieson, "From Silos to Systems: Issues in Clean Energy and Climate Change: DC microgrids: benefits and barriers," tech. rep., Yale School of Forestry & Environmental Sciences, 2010.

[9] Z. Ivanovic, B. Blanusa, and M. Knezic, "Power loss model for efficiency improvement of boost converter," in *Information, Communication and Automation Technologies (ICAT), 2011 XXIII International Symposium on*, pp. 1–6, IEEE, 2011.

[10] B. T. Lynch, "Under the hood of a dc/dc boost converter," in *TI Power Supply Design Seminar*, vol. 2009, 2008.

[11] V. Valtchev, A. Van den Bossche, J. Melkebeek, and D. Yudov, "Design considerations and loss analysis of zero-voltage switching boost converter," *IEE Proceedings-Electric Power Applications*, vol. 148, no. 1, pp. 29–33, 2001.

[12] J.-H. Kim, Y.-C. Jung, S.-W. Lee, T.-W. Lee, and C.-Y. Won, "Power loss analysis of interleaved soft switching boost converter for single-phase pv-pcs," *Journal of Power Electronics*, vol. 10, no. 4, pp. 335–341, 2010.

[13] F. Musavi, D. S. Gautam, W. Eberle, and W. G. Dunford, "A simplified power loss calculation method for pfc boost topologies," in *Transportation Electrification Conference and Expo (ITEC), 2013 IEEE*, pp. 1–5, IEEE, 2013.

[14] Y. Yu, W. Eberle, and F. Musavi, "A discontinuous boost power factor correction conduction loss model," in *Energy Conversion Congress and Exposition (ECCE), 2017 IEEE*, pp. 251–256, IEEE, 2017.

[15] C. Zhou, *Design and analysis of an active power factor correction circuit*. PhD thesis, Virginia Polytechnic Institute and State University, 1989.

[16] S. Lee, *Effects of input power factor correction on variable speed drive systems*. PhD thesis, Virginia Tech, 1999.

[17] C. Zhou, R. B. Ridley, and F. C. Lee, "Design and analysis of a hysteretic boost power factor correction circuit," in *Power Electronics Specialists Conference, 1990. PESC'90 Record., 21st Annual IEEE*, pp. 800–807, IEEE, 1990.

[18] T. A. Stuart and S. Ye, "Computer simulation of igbt losses in pfc circuits," *IEEE Transactions on Aerospace and Electronic Systems*, vol. 31, no. 3, pp. 1167–1173, 1995.

[19] X. Xie, Z. Zhou, J. Zhang, Z. Qian, and F. Peng, "Analysis and design of fully dcm clamped-current boost power-factor corrector with universal-input-voltage range," in *Power Electronics Specialists Conference, 2002. pesc 02. 2002 IEEE 33rd Annual*, vol. 3, pp. 1115–1119, IEEE, 2002.

[20] L. Huber, Y. Jang, and M. M. Jovanovic, "Performance evaluation of bridgeless pfc boost rectifiers," *IEEE Transactions on Power Electronics*, vol. 23, no. 3, pp. 1381–1390, 2008.